Z. Kristallogr. **219** (2004) 20–26

The system Cu_3AsS_4–Cu_3SbS_4 and investigations on normal tetrahedral structures

Arno Pfitzner* and Thomas Bernert

Universität Regensburg, Institut für Anorganische Chemie, Universitätsstraße 31, D-93040 Regensburg, Germany

Dedicated to Professor Dr. H.-L. Keller on the occasion of his 60th birthday

Received June 26, 2003; accepted August 12, 2003

X-ray diffraction / Powder diffraction structure analysis / Single crystal structure analysis / Thiometallate / Tetrahedral structures / Wurtzite structure type / Sphalerite structure type

Abstract. In order to develop a novel model to predict if a so called normal tetrahedral compound crystallizes in a *wurtzite*- or *sphalerite* superstructure type, the system Cu_3AsS_4–Cu_3SbS_4 was reinvestigated. A solid solution series was prepared and the mixed crystals were characterized by powder X-ray techniques. The crystal structures of $Cu_3As_{0.330}Sb_{0.670}S_4$, $Cu_3As_{0.736}Sb_{0.264}S_4$, and Cu_3AsS_4 were refined from single crystal X-ray data. The refinements converged to $R = 0.0209$, $wR2 = 0.0484$ ($Cu_3As_{0.330}Sb_{0.670}S_4$, 201 unique reflections, 15 parameters), $R = 0.0235$, $wR2 = 0.0596$ ($Cu_3As_{0.736}Sb_{0.264}S_4$, 218 reflections, 15 parameters), and $R = 0.0241$, $wR2 = 0.0669$ (Cu_3AsS_4, 721 reflections, 45 parameters). Z is 2 for all compounds. The volumes of the tetrahedra [MS_4] were calculated for the investigated compounds. In addition, the corresponding data were calculated for further solids from literature data. The volumes of the tetrahedra are used to separate compounds with a *sphalerite* type anion arrangement from compounds with hexagonal packed anions. A closer inspection of the tetrahedra volumes reveals a greater variation for one given material in the case of *wurtzite* type superstructures than for *sphalerite* type superstructures. A critical difference in the tetrahedra volumes is derived from these data.

Introduction

Normal tetrahedral structures have been investigated for a long time because of their interesting electrical and optical properties. *Parthé* has given easy valence electron rules in order to predict the composition of multinary compounds which crystallize in tetrahedral structures [1]. The cubic *sphalerite* structure type and the hexagonal *wurtzite* structure type are distinguished due to the packing of the anions. In ternary or multinary tetrahedral compounds the cation positions may be occupied in an ordered or in a statistic way. An ordered distribution causes a reduction of symmetry, e.g. leading to a tetragonal instead of a cubic cell for Cu_3SbS_4 (*famatinite*), whereas an orthorhombic cell instead of a hexagonal cell results for Cu_3AsS_4 (*enargite*) [2]. An even lower symmetry has been observed in some other cases.

The system Cu_3AsS_4–Cu_3SbS_4 is well investigated with respect to the formation of mixed crystals and thermal properties [3, 4]. According to powder data the structure of the mixed crystals $Cu_3As_xSb_{1-x}S_4$ changes at $x = 0.8$. For $x < 0.8$ the tetragonal *famatinite* type is observed, and for $x > 0.8$ the orthorhombic *enargite* type is found. Most of the former investigations concentrate on the stability of the different phases in the quasi-binary system. Kanazawa describes the evolution of the lattice parameters in the solid solution series $Cu_3As_xSb_{1-x}S_4$ [5]. Bernardini et al. examine the evolution of the d_{112}-values, the most intense reflection in the X-ray powder diagram. The d_{112} spacing increases linearly from *luzonite* to *famatinite* [6]. *Luzonite* is the arsenian homologue of *famatinite*.

In the literature some refinements of natural samples of *enargite* can be found [7–10]. However, these refinements cannot be used for deriving crystal chemical parameters since the natural samples may contain a manifold of elements. Only Karanović et al. determined the composition of their sample exactly by energy dispersive spectroscopy, it was $Cu_{3.074}As_{0.955}S_{3.971}$ [10].

The crystal structure of $Cu_3As_{0.685}Sb_{0.315}S_4$ was determined by *Marumo and Nowacki* in 1967 [11]. This composition was reinvestigated, as their data based on film methods.

To date it is not possible to predict which structure type will be formed by a normal tetrahedral compound with a given composition. Some authors suggest that the C cation in quaternary compounds A_2BCQ_4 (A = Cu, B = Mn, Fe, Co, Ni, Cd, C = Si, Ge, Sn, Q = S, Se) plays an important role [12]. However, despite numerous efforts, e.g. ref. [13], there is no concept available to de-

* Correspondence author
(e-mail: arno.pfitzner@chemie.uni-regensburg.de)

rive at least the arrangement of the anions from simple crystal chemical data, e.g. ionic radii of the constituent elements.

A novel approach to predict the preference for either a distorted hexagonal or a distorted cubic arrangement of the anions was recently described [14]. It became obvious that in Cu_3PS_4 (*enargite* type) the tetrahedra $[MS_4]$ (M = Cu, P) exhibit a significant difference of their volumes while in Cu_3SbS_4 the tetrahedra $[MS_4]$ (M = Cu, Sb) have about the same size.

Herein, we report our investigations of the system $Cu_3As_xSb_{1-x}S_4$. This system was chosen since Cu_3PS_4 and Cu_3SbS_4 do not form a solid solution series. Lattice constants and thermal behaviour of the mixed crystals are reported. In addition, selected compositions are characterized by single crystal X-ray structure determination. Thus, a precise information about the volumes of the tetrahedra $[MS_4]$ (M = Cu, As, Sb) is available. It is possible to derive critical volume ratios for the change from the cubic anion arrangement to the hexagonal packing from these data.

Experimental

Cu_3AsS_4 and Cu_3SbS_4 were prepared by annealing stoichiometric mixtures of the elements in evacuated, sealed quartz ampoules for two weeks at 590 °C. The products were homogenized between two annealing periods. The solid solutions $Cu_3As_xSb_{1-x}S_4$ ($x = 0.1$ to 0.9) were prepared from the end members by annealing stoichiometric mixtures at 595 °C for a total of four weeks. Again, the materials were ground between two annealing periods. After that time, no impurities were detected by X-ray powder diffraction.

Table 1. Crystallographic data for the X-ray structure determinations of $Cu_3As_{0.3}Sb_{0.7}S_4$, $Cu_3As_{0.3}Sb_{0.7}S_4$, and Cu_3AsS_4.[a]

Compound	$Cu_3As_{0.330}Sb_{0.670}S_4$	$Cu_3As_{0.736}Sb_{0.264}S_4$	Cu_3AsS_4
Formula weight/(g mol^{-1})	426.56	407.83	393.78
Crystal size/mm^3	0.12 0.10 0.08	0.11 0.09 0.09	0.32 0.20 0.18
Colour	black	black	black
Crystal system	tetragonal	tetragonal	orthorhombic
Space group	$I\bar{4}2m$ (no. 121)	$I\bar{4}2m$ (no. 121)	$Pmn2_1$ (no. 31)
Lattice constants/Å	$a = 5.353(1)$	$a = 5.315(1)$	$a = 7.399(1)$
	$c = 10.652(2)$	$c = 10.536(2)$	$b = 6.428(1)$
			$c = 6.145(1)$
Cell volume/Å^3, Z	305.2(1), 2	297.7(1), 2	292.3(1), 2
$\varrho_{X\text{-ray}}$/(g cm^{-3})	4.642	4.550	4.475
Diffractometer	STOE IPDS, MoK_α, $\lambda = 0.71073$ Å, oriented graphite monochromator		
Image plate distance /mm	60	55	60
φ-range/°, $\Delta\varphi$/°	$0° \le \varphi \le 112.5°$, 1.5	$0° \le \varphi \le 140°$, 2.0	$0° \le \varphi \le 173°$, 1.0
Absorption correction	Numerical, shape optimized with X-SHAPE [15]		
Irradiation time/image/min.	15	18	13
Temperature/°C	20	24	20
2 θ-range/°	$3.8 < 2\theta < 56.3$	$4.2 < 2\theta < 58.3$	$6.3 < 2\theta < 56.0$
hkl-range	$-6 \le h \le 6$	$-5 \le h \le 7$	$-9 \le h \le 9$
	$-6 \le k \le 6$	$-6 \le k \le 7$	$-8 \le k \le 8$
	$-13 \le l \le 9$	$-14 \le l \le 14$	$-7 \le l \le 8$
No. of reflections, $R_{int.}$	894, 0.0408	1257, 0.0398	2276, 0.0322
No. of independent reflections	201	218	721
No. of parameters	15	15	45
Program	SHELXL97 [16]		
$R1(I > 2\sigma)$, $R1$(all reflections)	0.0209, 0.0209	0.0235, 0.0235	0.0240, 0.0251
$wR(I > 2\sigma_I)$, wR(all reflections)[b]	0.0484, 0.0484	0.0596, 0.0596	0.0660, 0.0664
Weighting parameter a	0.0269	0.0390	0.0445
GooF	1.083	1.138	1.094
Largest difference peaks			
$\Delta\varrho_{max}$, $\Delta\varrho_{min}$/(e Å^{-3})	0.613, −0.630	0.739, −0.542	0.643, −0.597

a: Further details of the crystal structure investigations are available on request from the Fachinformationszentrum Karlsruhe, D-76344 Eggenstein-Leopoldshafen (Germany) (Fax: (+49)7247-808-666 (Dr. S. Höhler-Schlimm); E-mail: crysdata@fiz-karlsruhe.de), on quoting the depository numbers CSD-413348 ($Cu_3As_{0.330}Sb_{0.670}S_4$), CSD-413349 ($Cu_3As_{0.736}Sb_{0.264}S_4$), and CSD-413350 ($Cu_3AsS_4$).
b: Definition of $R1$ and wR:

$$R1 = \frac{\sum ||F_o| - |F_c||}{\sum |F_o|}, \qquad wR = \sqrt{\frac{\sum [w(F_o^2 - F_c^2)^2]}{\sum [w(F_o^2)^2]}}, \qquad GooF = \sqrt{\frac{\sum [w(F_o^2 - F_c^2)^2]}{n-p}}, \qquad w = 1/(\sigma^2(F_o^2) + (aF_o)^2).$$

Thermal analyses were carried out on a Setaram TMA 92 16.18 high temperature DSC in evacuated sealed quartz ampoules (inner diameter: 2.6 mm). X-ray powder diffraction data were collected in transmission setup on a STOE Stadi P equipped with Cu$K_{\alpha 1}$ radiation (Ge monochromator, Si as an external standard) and a linear PSD detector.

Single crystal X-ray diffraction data of $Cu_3As_{0.330}Sb_{0.670}S_4$ ($Cu_3As_{0.3}Sb_{0.7}S_4$), $Cu_3As_{0.736}Sb_{0.264}S_4$ ($Cu_3As_{0.7}Sb_{0.3}S_4$), and Cu_3AsS_4 were collected on a STOE IPDS. For all three compositions a numerical absorption correction was performed. The description of the crystal shapes was optimized with X-Shape [15]. The structures were solved by direct methods and refined against F^2 [16] with anisotropic displacement parameters for all atoms including an extinction parameter. The Flack parameter was used to check for the right setting of the non-centrosymmetric structures. It was 0.00(8) for $Cu_3As_{0.3}Sb_{0.7}S_4$, −0.01(5) for $Cu_3As_{0.7}Sb_{0.3}S_4$, and 0.07(2) for Cu_3AsS_4. This means, there was no evidence for inversion twinning. Crystallographic data and details of the refinements are collected in Table 1.

Results and discussion

Phase analytical investigations

The system $Cu_3As_xSb_{1-x}S_4$ has a two phase region at $x = 0.8$. Mixtures with $x < 0.8$ crystallize in the *famatinite* type, compositions with $x > 0.8$ crystallize in the *enargite* type. The sample with $x = 0.8$ contains both phases. Fig. 1c shows that the cell volume of the *famatinite* phase is close to the volume at $x = 0.7$, the volume of the *enargite* phase is close to the volume for $x = 0.9$. *Skinner* et al. found that the antimony richest *enargite* type composition in their studies was $Cu_3As_{0.874}Sb_{0.126}S_4$ (annealing temperature 500 °C). The same authors designated $Cu_3As_{0.691}Sb_{0.309}S_4$, grown at 425 °C, as the arsenic richest *famatinite* type composition they received in their studies [3]. *Sugaki et al.* determined the composition gap at temperatures of 400 °C, 500 °C, and 600 °C [4]. At 400 °C the immiscibility field reaches from about 2 to 38% Cu_3SbS_4. With higher temperatures the width of the field decreases, reaching from 6 to 33% Cu_3SbS_4 at 500 °C and 14–25% *famatinite* at 600 °C. For this temperature the authors reported the existence of small amounts of *tennantite-tetrahedrite* ($Cu_{12}As_4S_{13}$–$Cu_{12}Sb_4S_{13}$, both cubic, space group $I\bar{4}3m$ [17]). The evolution of the lattice parameters in the solid solution series *luzonite-famatinite* (both are tetragonal) was described by *Kanazawa* [5] and *Sugaki* et al. [4]. In both cases the authors report a linear variation over the whole composition range.

The orthorhombic lattice constants of *enargite* type solids can be transformed into tetragonal cell parameters using the following formulas:

$$a_{tet} = \frac{a_{ortho}}{\sqrt{2}}, \qquad b_{tet} = \frac{b_{ortho}}{\sqrt{3/2}},$$

$$\text{and} \quad c_{tet} = \sqrt{3} \cdot c_{ortho}.$$

The value for a_{tet} can thus be calculated from a_{ortho} and b_{ortho}. Here the average value of both data a_{tet} and b_{tet} is used since they are slightly different.

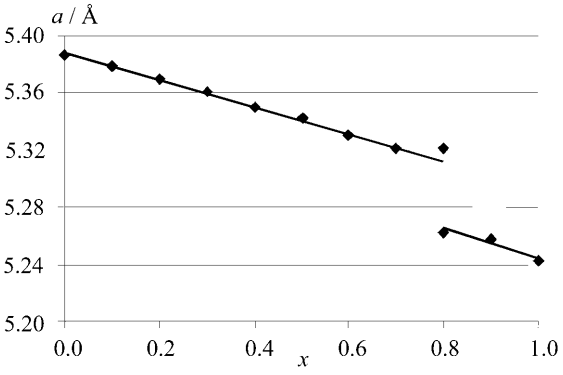

Fig. 1a. Tetragonal lattice parameter a_{tet} vs. the composition of the solid solution $Cu_3As_xSb_{1-x}S_4$.

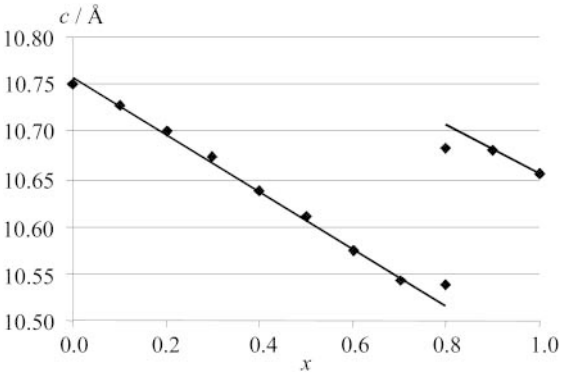

Fig. 1b. Tetragonal lattice parameter c_{tet} of the compositions in the system $Cu_3As_xSb_{1-x}S_4$.

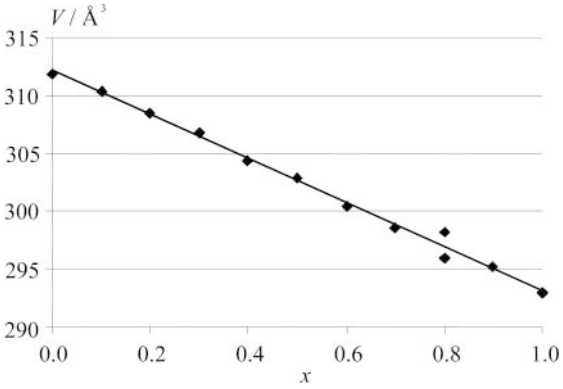

Fig. 1c. Cell volumes vs. composition in the system Cu_3AsS_4–Cu_3SbS_4.

The change of the structure with increasing As content around the composition gap becomes obvious from these data. The lattice constants a and c decrease linearly to $x = 0.8$ and then a falls to smaller values, while the parameter c jumps to higher values at this composition, see Fig. 1. The cell volume varies more or less linear over the whole composition range, because the contrary trends for c and a compensate each other.

The lattice constants of the *famatinite* type compositions are in good agreement with the data published in refs. [4, 5].

The ratio c/a decreases linearly with an increasing content of arsenic. Its value declines from the ideal tetragonal ratio $c/a = 2$, which is nearly reached in Cu_3SbS_4 (c/a

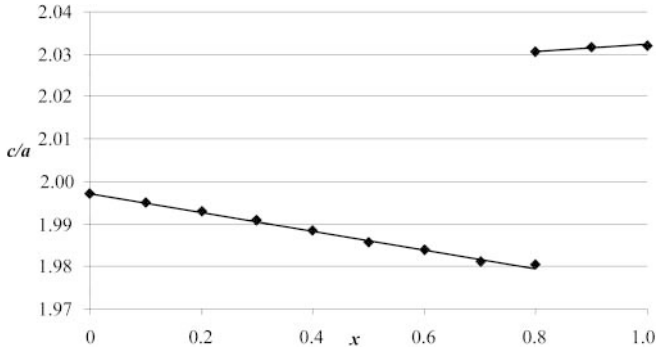

Fig. 2. Development of the *c/a* ratios with increasing content of As in $Cu_3As_xSb_{1-x}S_4$ (data for $x \geq 0.8$ are transferred to the tetragonal metric, *vide supra*).

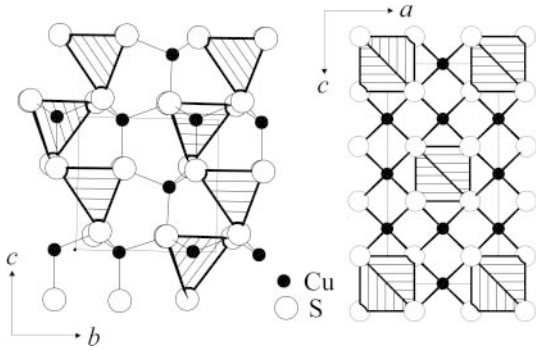

Fig. 4. Orthorhombic Cu_3AsS_4 (left) compared to tetragonal $Cu_3As_{0.7}Sb_{0.3}S_4$ (right). As and Sb are located in the tetrahedra. Note the different tetrahedral sizes the *enargite* structure while the different tetrahedra in $Cu_3As_{0.7}Sb_{0.3}S_4$ have almost the same size.

$= 1.997$) to $c/a = 1.981$ in $Cu_3As_{0.7}Sb_{0.3}S_4$. Contrary to the linear behaviour for the series *famatinite-luzonite* [5] a discontinuity is found for the series *famatinite-enargite* at $x = 0.8$. The *enargite* type compositions have ratios $c/a > 2.03$, see Fig. 2. Again, the values of the *famatinite* compositions agree very well.

The splitting of the reflections in the powder diffraction patterns depends strongly on the *c/a* ratio. This splitting becomes more and more evident with an increasing As content due to the increasing structural distortions.

Famatinite is reported to melt congruently at 627 °C [18]. The melting points reported for *enargite* are not unique. Some authors suggest the congruent melting of *enargite* at 655 °C [19], and 674 °C [20] while others report a particular decomposition at 600 °C [4]. A detailed survey of the contradictory results is given by *Müller and Blachnik* who report the melting point of Cu_3AsS_4 as 694 °C [21].

Melting points of the mixed crystals $Cu_3As_xSb_{1-x}S_4$ were determined by DTA measurements in order to investigate the thermal behaviour of the system Cu_3AsS_4–Cu_3SbS_4. The compositions were heated twice to 1000 °C with a rate of 10 °C per minute and cooled again with the same rate. The second heating cycle was performed in order to examine if the substances melt congruently.

The melting points for Cu_3SbS_4 (632 °C) and Cu_3AsS_4 (692 °C) are in good agreement with refs. [18, 21]. The melting points of the mixed crystals increase linearly with an increasing content of As, as shown in Fig. 3.

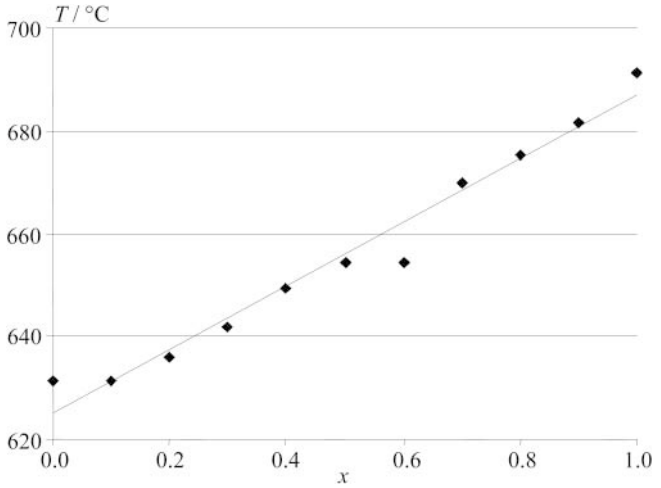

Fig. 3. Melting points in the system $Cu_3As_xSb_{1-x}S_4$.

The thermal effects in the two heating cycles are identical within the tolerances. An X-ray powder diffraction diagram was recorded for $Cu_3As_{0.5}Sb_{0.5}S_4$ after melting. The diffraction data show the coexistence of the *famatinite* type and a second phase belonging to the $Cu_{12}As_4S_{13}$–$Cu_{12}Sb_4S_{13}$ series. We also recognized a decomposition upon heating the end members to 700 °C. These results are in agreement with the results of *Sugaki et al.*, who investigated the system Cu_3AsS_4–Cu_3SbS_4 at a temperature of 600 °C. They found a particular decomposition into the tennantite-tetrahedrite system, too [4]. *Müller and Blachnik* report that heating Cu_3AsS_4 above the melting point of *enargite* increases the amount of by-products [21].

Single crystal investigations

The results of the crystal structure analyses are collected in tables 2–5. The compounds consist of corner sharing tetrahedra [CuS_4] and [(As/Sb)S_4] in a ratio 3 : 1. As and Sb are statistically distributed on the M^V positions.

During the refinement only one common position and common displacement parameters for Sb and As were considered. The occupancies of Sb and As were constrained to result in fully occupied positions.

We showed recently for Cu_3PS_4 and Cu_3SbS_4 that in Cu_3PS_4 the tetrahedra [CuS_4] and [PS_4] differ significantly in size whereas they have about the same size in Cu_3SbS_4. The higher symmetrical *sphalerite* structure type cannot be built if the differences between different tetrahedra are too large. In order to verify this idea, the system Cu_3AsS_4–Cu_3SbS_4 was investigated with respect to this assumption. The volumes of the tetrahedra were calculated from the lengths of the edges (see Fig. 5 for assignment)

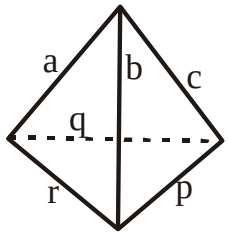

Fig. 5. Labelling of the tetrahedral edges.

Table 2. Atomic parameters (e.s.d.s) and U_{eq}[a] (in Å^2) for $Cu_3As_{0.3}Sb_{0.7}S_4$ and $Cu_3As_{0.7}Sb_{0.3}S_4$.

Atom	Wyckoff pos.	Occ.	x	y	z	U_{eq}
$Cu_3As_{0.3}Sb_{0.7}S_4$						
Sb	2*a*	0.736(3)	0	0	0	0.0119(2)
As	2*a*	0.264	0	0	0	0.0119(2)
Cu1	4d		0.5	0	0.25	0.0233(2)
Cu2	2b		0.5	0.5	0	0.0230(3)
S	8*i*		0.2501(1)	*x*	0.1273 (1)	0.0161(3)
$Cu_3As_{0.7}Sb_{0.3}S_4$						
Sb	2*a*	0.330(2)	0	0	0	0.0096(2)
As	2*a*	0.670	0	0	0	0.0096(2)
Cu1	4d		0.5	0	0.25	0.0211(2)
Cu2	2b		0.5	0.5	0	0.0210(2)
S	8*i*		0.2439(1)	*x*	0.1250 (1)	0.0143(3)

a: U_{eq} is defined as one third of the trace of the orthogonalized U_{ij} tensor.

Table 3. Anisotropic displacement parameters U_{ij} (in Å^2) for $Cu_3As_{0.3}Sb_{0.7}S_4$ and $Cu_3As_{0.7}Sb_{0.3}S_4$.

Atom	$U_{11} = U_{22}$	U_{33}	U_{12}	$U_{13} = U_{23}$
$Cu_3As_{0.3}Sb_{0.7}S_4$				
Sb1	0.0119(2)	0.0120(3)	0	0
As1	0.0119(2)	0.0120(3)	0	0
Cu2	0.0224(3)	0.0251(4)	0	0
Cu3	0.0228(3)	0.0233(5)	0	0
S4	0.0156(4)	0.0173(7)	0.0004(3)	0.0008(2)
$Cu_3As_{0.7}Sb_{0.3}S_4$				
Sb	0.0090(2)	0.0000(2)	0	0
As	0.0090(2)	0.0000(2)	0	0
Cu1	0.0202(3)	0.0000(3)	0	0
Cu2	0.0205(3)	0.0000(4)	0	0
S	0.0137(5)	0.0154(6)	0.0005(2)	0.0004(2)

Table 4. Atomic parameters (e.s.d.s) and U_{eq} [a] (in Å^2) for Cu_3AsS_4.

Atom	Wyckoff pos.	x	y	z
As	2*a*	0	0.1726(1)	0.0014(1)
Cu1	2*a*	0	0.8467(1)	0.5016(2)
Cu2	4*b*	0.7523(1)	0.6745(1)	0.0097(1)
S1	2*a*	0	0.1777(2)	0.3589(3)
S2	2*a*	0	0.8517(2)	0.8763(3)
S3	4*b*	0.7436(1)	0.6648(1)	0.3811(2)

a: U_{eq} is defined as one third of the trace of the orthogonalized *Uij* tensor.

with the formula [22]

$$V = \left(\frac{1}{288} \cdot \begin{vmatrix} 0 & r^2 & q^2 & a^2 & 1 \\ r^2 & 0 & p^2 & b^2 & 1 \\ q^2 & p^2 & 0 & c^2 & 1 \\ a^2 & b^2 & c^2 & 0 & 1 \\ 1 & 1 & 1 & 1 & 0 \end{vmatrix} \right)^{\frac{1}{2}} .$$

We have calculated the average volumes of all tetahedra in the compounds under discussion. From the volumes V_i of the distinct tetrahedra i in a compound we have calculated the following values:

- $\overline{V_i}$, the average value of all tetrahedral volumes
- ΔV_i, the difference of the average volume $\overline{V_i}$ from the volume V_i, $\Delta V_i = V_i - \overline{V_i}$
- $\overline{\Delta V_i}$, the average value of ΔV_i.

The values are given in Table 6. The data for Cu_3PS_4 and Cu_3SbS_4 were calculated from ref. [14].

Plotting ΔV_i of the tetrahedra [MS_4] (M = (As_xSb_{1-x})) of the compositions with $x = 0.0$, 0.3, 0.7, and 1.0 against the composition provides a linear dependence, shown in Fig. 6.

For Cu_3PS_4 $\overline{\Delta V_i}$ is quite high as expected. On the other hand for *sphalerite* type structures we receive small values. $\overline{\Delta V_i}$ for *enargite* is slightly bigger as compared to the *sphalerite* related compositions.

If we compare the average values $\overline{\Delta V_i}$ for the system Cu_3AsS_4–Cu_3SbS_4, we expect a minimum at about $x = 0.4$. This is, because the tetrahedra [SbS_4] are larger than the polyhedra [CuS_4], but the tetrahedra [AsS_4] are smaller. If Sb is substituted by As, there exists a composition where the tetrahedra [(As_xSb_{1-x})S_4] reach the same

Table 5. Anisotropic displacement parameters U_{ij} (in Å^2) for Cu_3AsS_4.

Atom	U_{11}	U_{22}	U_{33}	U_{12}	U_{13}	U_{23}
As	0.0103(3)	0.0078(3)	0.0095(3)	0	0	−0.0001(3)
Cu1	0.0222(4)	0.0195(3)	0.0187(4)	0	0	0.0025(5)
Cu2	0.0213(3)	0.0183(3)	0.0197(6)	0.0013(1)	−0.0008(2)	0.0011(4)
S1	0.0130(7)	0.0127(7)	0.0070(7)	0	0	0.0010(5)
S2	0.0134(6)	0.0083(5)	0.0133(7)	0	0	−0.0001(6)
S3	0.0110(5)	0.0105(5)	0.0145(9)	0.0017(3)	0.0008(3)	−0.0004(3)

Table 6. Volumes of the different tetrahedra in the investigated compositions.

Compound	ΔV_i of $[Cu_1S_4]$	ΔV_i of $[Cu_2S_4]$	ΔV_i of $[MS_4]$	$\overline{\Delta V_i}$
Cu_3PS_4	10.4	5.1	−20.6	10.3
Cu_3AsS_4	5.1	2.7	−10.4	5.2
$Cu_3As_{0.7}Sb_{0.3}S_4$	5.0	0.0	−5.0	3.3
$Cu_3As_{0.3}Sb_{0.7}S_4$	1.8	−1.9	1.9	1.8
Cu_3SbS_4	−0.4	3.1	6.6	3.3

Table 7. $\overline{V_i}$ for different compounds.

Compound	Space-group	$\overline{\Delta V_i}$	ref.	Structure-Type
Cu_2GeS_3	Cc	3.7	[23]	sst [a]
Cu_2SnS_3	$I\bar{4}2m$	2.3	[24]	sst
Cu_3SbSe_4	$I\bar{4}2m$	5.8	[17]	sst
$CuFeS_2$	$I\bar{4}2d$	2.4	[25]	sst
Cu_4TiS_4	$I\bar{4}2m$	2.2	[26]	sst
Cu_2SiS_3 (LT)	Cc	7.3	[27]	sst
Li_3AsO_4	$Pmn2_1$	15.2	[28]	wst [b]
Li_3PO_4	$Pmna$	21.4	[29]	wst
$AlLiSe_2$	$Pmn2_1$	10.0	[30]	wst
Ag_3AsS_4	$Pmn2_1$	15.0	[31]	wst
Cu_2SiS_3 (HT)	$Cmc2_1$	8.6	[32]	wst

a: sst: *sphalerite* superstructure type
b: wst: *wurtzite* superstructure type

size as the polyhedra $[CuS_4]$. This is at about $x = 0.4$, cf. Fig. 6. With increasing amounts of As the tetrahedra $[(AsSb)S_4]$ become smaller and $\overline{\Delta V_i}$ increases again.

Structural data from the literature were also evaluated in order to verify these findings. From Table 7 one can see that *sphalerite* type compounds have significantly smaller $\overline{\Delta V_i}$ values than *wurtzite* type compounds. The question arises for a "critical" $\overline{\Delta V_i}$ that separates *sphalerite* and *wurtzite* type compounds from each other.

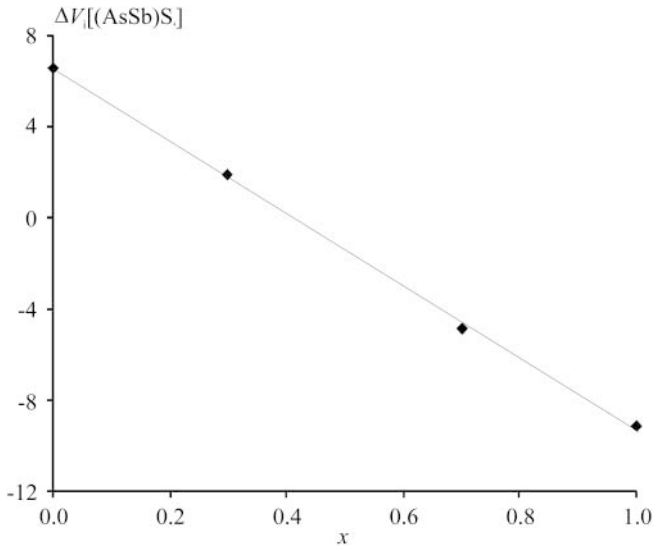

Fig. 6. Plot of ΔV_i of the tetrahedra $[MS_4]$ (M = As, (AsSb), Sb) against the composition of $Cu_3As_xSb_{1-x}S_4$.

The largest $\overline{\Delta V_i}$ we calculated for a *famatinite* type compound was 8.8 for $Cu_4NiSi_2S_7$. The structure was solved by *Schäfer* et al. [33]. We refined the structure again [34] in order to verify this relatively large $\overline{\Delta V_i}$ and observed $\overline{\Delta V_i} = 8.5$. This difference is not remarkable. The smallest $\overline{V_i}$ for an *enargite* type compound was found for *enargite* itself with $\overline{\Delta V_i} = 5.2$.

This means that there is an intermediate range where either one or the other packing can be realized, cf. also Cu_3SiS_3 [27, 32]. To date, our model fits crystal structures of chalcogenides quite well. However, an inspection of the structures of more ionic compounds, e.g. ternary nitrides, shows that different critical parameters have to be derived here for a broader applicability of our approach.

Acknowledgments. We thank the Fonds der Chemischen Industrie FCI and the Bundesministerium für Bildung und Forschung BMBF for valuable financial support.

References

[1] Parthé, E.: Wurtzite and Sphalerite Structures. In: *Crystal Structures of Intermetallic Compounds*. (Eds. J. H. Westbrook, R. L. Fleischer), J. Wiley and Sons, New York, 2000.
[2] Parthé, E.; Yvon, K.; Deitch, R. H.: The Crystal Structure of Cu_2CdGeS_4 and Other Quaternary Normal Tetrahedral Structure Compounds. Acta Crystallogr. B**25** (1969) 1164–1174.
[3] Luce, F. D.; Tuttle, C. L.; Skinner, B. J.: Studies of Sulfosalts of Copper: V. Phases and Phase Relations in the System Cu–Sb–As–S between 350° and 500 °C. Econ. Geol. **72** (1977) 271–289.
[4] Sugaki, A.; Kitakaze, A.; Shimizu, Y.: Phase relations in the Cu_3AsS_4–Cu_3SbS_4 join. Science reports of the tohoku university, ser. 3 **15(2)** (1982) 257–271.
[5] Kanazawa, Y.: Synthesis and lattice constants of luzonite-famatinite crystals. Bull. Geol. Surv. Japan **35(1)** (1984) 13–17.
[6] Bernardini, G. P.; Tanelli, G.; Trosti, R.: Relazioni di fase nel sistema Cu_3AsS_4–Cu_3SbS_4. Soc. Italian Miner. Petrol. **29(2)** (1973) 281–296.
[7] Pauling, L.; Weinbaum, S.: The Crystal Structure of Enargite, Cu_3AsS_4. Z. Kristallogr. **88** (1934) 48–53.
[8] Adiwidjaja, G.; Löhn, J.: Strukturverfeinerung von Enargit, Cu_3AsS_4. Acta Crystallogr. B**26** (1970) 1878–1879.
[9] Henao, J. A.; Díaz de Delgado, G.; Delgado, J. M.: Single-crystal structure refinement of enargite $[Cu_3AsS_4]$. Mater. Res. Bull. **29(11)** (1994) 1121–1127.
[10] Karanović, Lj.; Cvetković, Lj.; Poleti, D.; Balić-Žunić, T.; Makovicky, E.: Crystal and absolute structure of enargite from Bor (Serbia). Neues Jahrb. Mineral., Monatsh. **6** (2002) 241–253.
[11] Marumo, F.; Nowacki, W.: A Refinement of the Crystal Structure of Luzonite, Cu_3AsS_4. Z. Kristallogr. **124** (1967) 1–8.
[12] Schäfer, W.; Nitsche, R.: Tetrahedral quaternary chalcogenides of the type Cu_2-II-IV-$S_4(Se_4)$. Mater. Res. Bull. **9** (1974) 645–654.
[13] O'Keeffe, M.; Hyde, B. G.: Non-bonded interactions and the crystal chemistry of tetrahedral structures related to the wurtzite type (B4). Acta Cryst. B**34** (1978) 3519–3528.
[14] Pfitzner, A.; Reiser, S.: Refinement of the crystal structure of Cu_3PS_4 and Cu_3SbS_4 and a comment on normal tetrahedral structures. Z. Kristallogr. **217** (2002) 51–54.
[15] STOE & Cie GmbH Darmstadt, 1996, 1997, Crystal optimisation for Numerical Absorption Correction.
[16] Sheldrick, G. M.: SHELXL 97, Programm zur Kristallstrukturverfeinerung, Universität Göttingen, 1997.
[17] Pfitzner, A.; Evain, M.; Petricek, V.: $Cu_{12}Sb_4S_{13}$: A Temperature-Dependent Structure Investigation. Acta Crystallogr. B**53** (1997) 337–345.
[18] Skinner, B. J.; Luce, F. D.; Mackovicky, E.: Studies in the Sulfosalts of Copper III. Phases and Phase Relations in the System Cu–Sb–S. Econ. Geol. **67** (1972) 924–938.
[19] Wernick, J. H.; Benson, K. E.: New semiconducting ternary compounds. J. Phys. Chem. Solids **3** (1957) 157–158.

[20] Rikel', M.; Harmelin, M.; Prince, A.: Arsenic-Copper-Sulfur. In: *Ternary Alloys Vol. 10* (Eds. G. Petzow, G. Effenberg, F. Aldinger), VCH Verlagsgesellschaft mbH, Weinheim, 1994.

[21] Müller, A.; Blachnik, R.: Reactivity in the system copper-arsenic-sulfur I. The formation of Cu_3AsS_4, enargite. Thermochim. Acta **387** (2002) 153–171.

[22] Bronstein, I. N.; Semendjaev, K. A.: Taschenbuch der Mathematik, Verlag Harry Deutsch, Zürich 1969.

[23] De Chalbaud, L. M.; Díaz de Delgado, G.; Delgado, J. M.; Mora, A. E.; Sagredo, V.: Synthesis and single-crystal structural study of Cu_2GeS_3. Mater. Res. Bull. **32(10)** (1997) 1371–1376.

[24] Chen, X.-a.; Wada, H.; Sato, A.; Mieno, M.: Synthesis, electrical conductivity, and crystal structure of $Cu_4Sn_7S_{16}$ and structure refinement of Cu_2SnS_3. J. Solid State Chem. **139** (1998) 144–151.

[25] Kratz, T.; Fuess, H.: Simultane Strukturbestimmung von Kupferkies und Bornit an einem Kristall. Z. Kristallogr. **186** (1989) 167–169.

[26] Klepp, K. O.; Gurtner, D.: Synthesis and crystal structure of Cu_4TiS_4: a novel chalcogenide with tetrahedrally coordinated titanium. J. Alloys Compd. **243** (1996) 19–22.

[27] Chen, X.-a.; Wada, H.; Sato, A.; Nozaki, H.: Synthesis, structure and electronic properties of Cu_2SiQ_3 (Q = S, Se). J. Alloys Compd. **290** (1999) 91–96.

[28] Elfakir, A.; Wallez, G.; Quarton, M.; Pannetier, J.: Polymorphism of Li_3AsO_4 and structure refinement of its low temperature form. Phase Transitions **45** (1993) 281–288.

[29] Wang, B.; Chakoumakos, B. C.; Sales, B. C.; Kwak, B. S.; Bates, J. B.: Synthesis, crystal structure, and ionic conductivity of a polycristalline lithium phosphorus oxynitride with the γ-Li_3PO_4. J. Solid State Chem. **115** (1995) 313–323.

[30] Kim, J.; Hughbanks, T.: Synthesis and structures of new ternary aluminium chalcogenides: $LiAlSe_2$, α-$LiAlTe_2$, and β-$LiAlTe_2$. Inorg. Chem. **39** (2000) 3092–3097.

[31] Rosenstingl, J.: Synthese und Kristallstrukturbestimmung von Ag_3AsS_4 (ein Vertreter des Strukturtyps Enargit, Cu_3AsS_4). Oesterreische Akademie der Wissenschaften, Mathematisch-Naturwissenschaftliche Klasse, Sitzungsberichte **130** (1993), 27–30.

[32] Parthé, E.; Garin, J.: Zinkblende- und Wurtzitüberstrukturen bei ternären Chalkogeniden der Zusammensetzung $1_2 4 6_3$. Monatsh. Chem. **102** (1971) 1197–1208.

[33] Schäfer, W.; Scheunemann, K.; Nitsche, R.: Crystal structure and magnetic properties of $Cu_4NiSi_2S_7$. Mater. Res. Bull. **15** (1980) 933–937.

[34] $Cu_4NiSi_2S_7$: STOE IPDS, Mo-Anode, oriented graphite monochromator, $\lambda = 0.71073$ Å, refinement (SHELX97 [16]), numerical absorption correction, shape optimized with X-SHAPE [15], 0.28 0.12 0.09 mm^3, monoclinic, space group $C2$, $Z = 2$, $T = 20$ °C, $a = 11.561$ (2) Å, $b = 5.324$ (1) Å, $c = 8.188$ (2) Å, $\beta = 98.71°$, $V = 498.2$ (2) Å^3, $4.2 < 2\theta < 58.6$, $\varrho_{\text{X-ray}} = 3.956$ g cm^{-3}, 5996 reflections ($R_{\text{int}} = 0.0328$), 1300 independent reflections, $R1(\text{I} > 2\sigma) = 0.0318$, $R1$(all reflections) $= 0.0325$, wR ($I > 2\sigma_{\text{I}}$) $= 0.0940$, wR (all reflections) $= 0.0945$, 65 parameters, $\Delta\varrho_{\max} = 0.614$ e Å^{-3}, $\Delta\varrho_{\max} = -0.555$ e Å^{-3}. Further details of the crystal structure investigations are available on request from the Fachinformationszentrum Karlsruhe, D-76344 Eggenstein-Leopoldshafen (Germany) (Fax: (+49)7247-808-666 (Dr. S. Höhler-Schlimm); E-mail: crysdata@fiz-karlsruhe.de), on quoting the depository number CSD-413347.